2.1 INTRODUCTION

The present chapter deals with the description of raw materials, processing techniques used and experimental techniques followed during the course of investigation. The chapter is divided into three sections. The first section describes in detail about the selection of materials, processing techniques, parameters used for processing and heat treatment given to the samples. It also describes powder characterization, procedure for printing parts and the process parameters utilised to print samples with varied build orientations of 0^o, 45^o and 90^o. The second section deals with the characterization of processed parts and different experimental testing methods used for testing the samples. Microstructural characterization of additive manufactured (AM) and conventional samples in as-built (AB) and heat-treated (HT) conditions are also described. The geometry of tensile, wear and erosion, corrosion samples and parameters for tensile, wear, erosion and corrosion testing are discussed in detail. In the third section, the details of fractography of tensile and fatigue-tested samples by SEM, analysis of worn and eroded samples by SEM, EDS and AFM is described. Also, the analysis of corroded samples by SEM, EDS and XPS is discussed.

2.2 MATERIALS

Gas atomized maraging steel (M300 grade) powder was procured from Renishaw Additive Manufacturing Solutions Centre, Pune, India. Conventionally manufactured (as cast and hot rolled) maraging steel of M300 grade was procured from Bharat Aerospace Metals, Mumbai, India. Composition of both forms of maraging steel (gas atomized powder and conventionally manufactured maraging steel) were found to be within the range as per the specifications for 300-grade maraging steel. The chemical compositions of M300 maraging steel powder and conventionally manufactured (CM) maraging steel are given in Table 2.1 and are found to be comparable.

Table 2.1 Chemical composition of maraging steel (M300) used in the present work**.**

Element (%)	Ni	Co	Mo	Ti	Al	Si	Mn	P	S	C	Fe
Conventio -nal steel (M300)	18	9.2	4.8	0.5	0.01	0.01	0.01	0.003	0.002	0.004	67.5
Gas atomized powder (M300)	18.2	9.1	4.9	0.5	0.01	0.04	0.1	0.01	0.01	0.02	67.1

2.3 PROCESSING OF POWDERS

2.3.1 Powder Bed Fusion using Laser Beam (PBF-LB)

3D models of plates of 55 x 55 x 5 mm^3 and rods of 110 mm length and 13 mm diameter in 0^o, 45^o and 90^o orientations with block and contour support for STL file generation in Materialise Magics 23 software were made as shown in Fig. 2.1(a). Further for processing of 3D model of plates and rods in 0^o, 45^o and 90, 3D printer which prints via powder bed fusion using laser beam (PBF-LB) (Make: Renishaw AM250) was used. Renishaw AM250 system has a build chamber of 250 x 250 x 300 mm^3 and uses a 400W Ytterbium fibre laser. The system is equipped with a vacuum unit along with inlet and outlet for argon gas to maintain oxygen at the bottom, a re-coater to spread powder and a laser optical system to scan the powder layer by layer. During the processing of powder, the dispenser moves up and the build chamber and collector go down to achieve the processed product height. Figs. 2.1 (b and c) present schematic view of the components of the Renishaw AM250 system and the AM250 Renishaw powder bed system.

Initially, inert gas (argon) was purged to maintain inert atmosphere with oxygen up to 1000 ppm. After this, the required amount (based on layer thickness) of powder was spread on the base plate by re-coater, using optical controller software (OCS). The laser

beam was used to scan the powder with strip hatch pattern having width of 14 mm to fuse the powder.

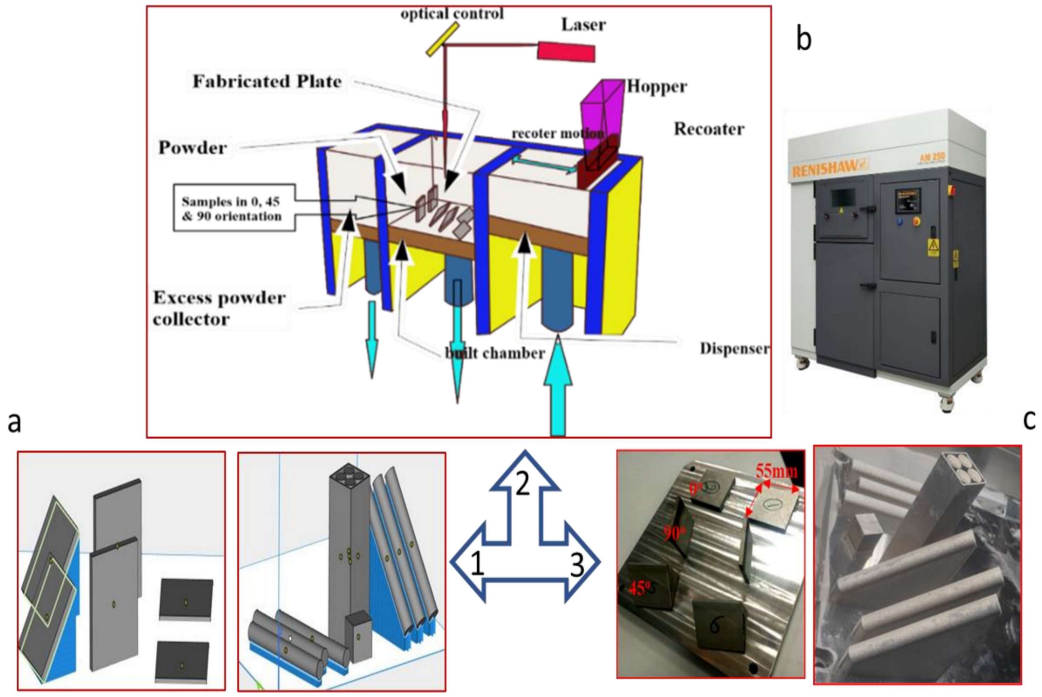

Fig. 2.1 (a) 3D models of plates and rods with support structure, (b) Schematic view and Renishaw AM250 PBF-LB system and (c) Processed plates and rods with support structure and base plate in different orientations.

This process was repeated several times to build the required plates in different orientations. Optimized process parameters were obtained from Ansys Additive software, to have better part density. Process parameters used to manufacture the plates in 0^o, 45^o and 90^o build orientations are: Laser Power (P): 400 W, laser wavelength (λ): 1070 nm, laser spot diameter (D): 0.08 mm, hatch spacing (d): 0.08 mm, scan speed (v): 2 m/s, layer thickness (t): 0.04 mm, inter layer rotation: 67^o, build rate: 15 cm^3/h. Energy density (E) is also an important parameter in powder bed laser processing. It relates the laser power (P), scan speed (v), layer thickness (t) and hatch spacing (d) and can be related by Equation (2.1) [15].

$$E = \frac{P}{vdt} \quad (2.1)$$

In the present study, energy density of 62.5 J/mm^3 was used to build plates with high density. Additive manufactured samples (AM) were separated by wire electro-discharge machining (EDM) from mild steel base plates.

2.4 INITIAL CHARACTERIZATION

2.4.1 Surface Roughness and Relative density

Surface roughness of plates and rods built in different orientations was measured by surface profilometer (SU-410 Mitutoyo). The CONTECH density balance was used to get relative density of different AM samples as per Equation (2.2) [109]. Weight of the plates in air and weight of plates in water were used to calculate density.

$$\frac{\rho(slm)}{\rho(standard)}\% = \frac{\rho(water)\times Wslm(air)}{\rho(standard)\times[Wslm(air)-Wslm(water)]} \times 100 \quad (2.2)$$

where $\rho_{(slm)}$ is density of AM sample, $\rho_{(standard)}$ is density of maraging steel, $\rho_{(water)}$ is density of water, $W_{slm(air)}$ is weight of AM sample in air and $W_{slm(water)}$ is weight of AM sample in water. Three readings were taken for each sample and average was taken to get the relative density of AM samples in different orientations.

2.4.2 Heat Treatment and Microstructural characterization

From the as-built AM processed plates of different orientations and CM plates, specimens of 7×7×5 mm^3 were machined out for subsequent heat treatments (solution treatment plus aging treatment). These specimens were subjected to a solution treatment at 815^{o}C for 1 h in inert atmosphere (N_2), cooled in air. They were subsequently aged at 520^{o}C for 5 h and cooled in air as depicted in Fig.2.2. For achieving good tensile, fatigue, wear and erosion properties, aging for long duration of 5 h was planned [110]. The same

heat treatment was also given for the characterization of corrosion behaviour of the M300 specimens in both additive manufactured and conventional specimens. The designations of samples used for testing is given in Table 2.2.

Table 2.2 Designation of different samples used for testing.

Sample conditions	Sample designation	Explanation
Additive Manufactured (AM)	0° AB	Additive manufactured as built sample in 0° orientation
	45° AB	Additive manufactured as built sample in 45° orientation
	90° AB	Additive manufactured as built sample in 90° orientation
Additive Manufactured and heat treated (AM-HT)	0° HT	Heat treated Additive manufactured sample in 0° orientation
	45° HT	Heat treated Additive manufactured sample in 45° orientation
	90° HT	Heat treated Additive manufactured sample in 90° orientation
Conventionally Manufactured (CM)	CM	As received conventionally manufactured sample
	CM-HT	Conventionally manufactured and heat-treated sample

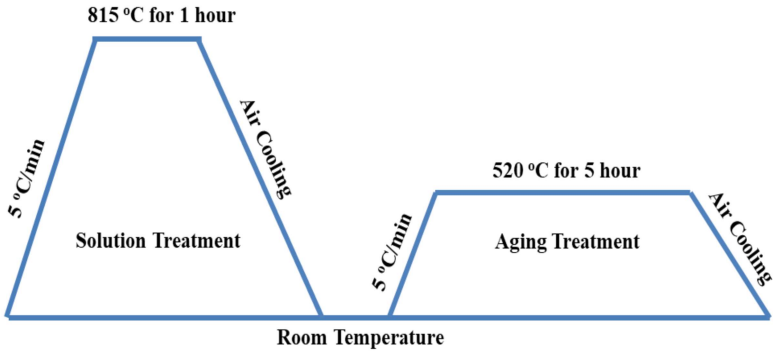

Fig. 2.2 Heat Treatment (HT) adopted for the present M300 maraging steel.

Phase analysis of samples were done by using X-ray Diffraction Analysis (XRD) by Empyrean PANalytical, High Resolution X-Ray Detector (HR XRD) with Co source (λ=1.7A°). Phase scan parameters selected were: scan rate of 5°/min and 2Θ range (20°-

120°). Volume fraction of different phases was calculated by relative intensity method as given by Equation 2.3 [111].

$$Wp = \frac{P}{\sum Pi} \times 100 \qquad (2.3)$$

p = relative intensity of phase, p and $\sum pi$ = sum of relative intensity of all phases.

Residual stress experiments were performed using HR XRD. Using $Sin^2\psi$ method, the residual stress values were determined [112]. A high angle (range from, min. start angle (2Θ) ~ 94.32° to max. end angle (2Θ) ~ 104.23°) bcc peak (211) was taken for analysis. The experiments were performed with step size of 0.02, time per step as 2 s.

Microstructural characterization was performed by first polishing the samples, then applying etchant of 5% Nital to reveal microstructure and using the DFC295, Leica, 2015 optical microscope and scanning electron microscope (Zeiss). For transmission electron microscopy (TEM), samples were machined using slow speed diamond cutter from the samples in different conditions. Thickness of samples were reduced from 1 mm to 50 μm using abrasive papers of 200, 400, 800, 1200,1500, 2500 mesh and then the thin samples were punched into 3 mm diameter discs by punching die for electro polishing. Twin jet polisher (Tenupol-5, Struers), with holder, was used for electro polishing. TEM specimens were prepared by electro polishing with a solution of 10% perchloric acid and 90% methanol at -30°C at 20 V. Transmission electron microscope (FEI Technai $20G^2$), operating at 200 kV was used for microstructural examination at high magnifications and identification of phases by selected area diffraction (SAD).

2.5 MECHANICAL BEHAVIOUR

2.5.1. Hardness and Tensile behaviour

As-built (AB) and heat-treated (HT) specimens of 7×7×5 mm^3 were polished and Micro hardness tester (LECO: LV 248AT) with 500 gf load and 10 s dwell time was used to obtain hardness values of all samples. Seven readings per sample were taken and average of these values was taken as hardness of that sample. Sub-size flat tensile samples with gauge length of 15 mm, width of 5 mm and thickness of 2 mm were machined out from the plates and were polished using SiC paper as shown in Figs. 2.3 (b and c).

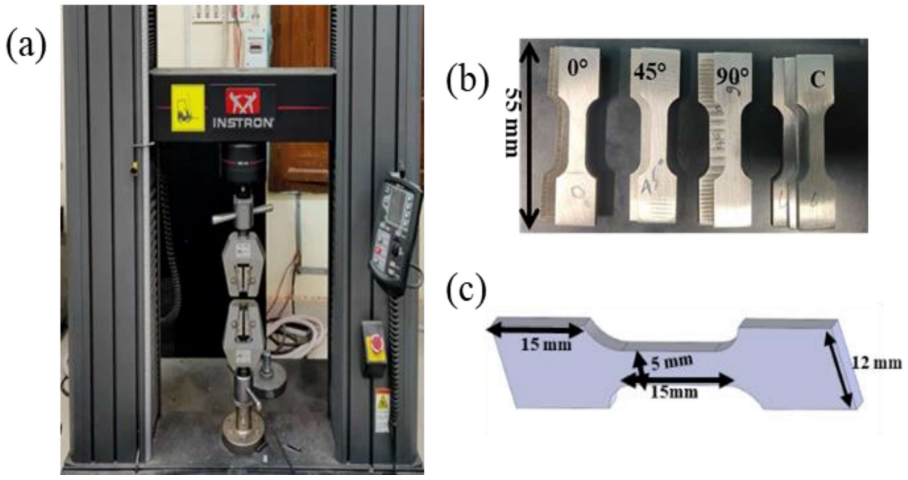

Fig. 2.3 (a) 100kN Universal Testing Machine (b) Subsize polished flat tensile samples built in orientation of 0°, 45°, 90° and CM sample (c) Dimensions of subsize tensile sample.

Tensile testing was performed using a 100 kN Universal testing machine (INSTRON 5982) shown in Fig. 2.3(a), at a strain rate of 10^{-3} s^{-1}. For repeatability of tensile results, two samples were tested for each condition. Fracture surfaces of the tested specimens were analyzed using scanning electron microscope operating at 20kV. The variation of tensile properties such as strength and ductility with orientation is defined as strength anisotropy (A_{IP}) and elongation anisotropy index (δ) respectively. Strength anisotropy

and elongation anisotropic index of additive manufactured (AM) as built and heat-treated (HT) samples were calculated by Equation (2.4 and 2.5) [113-115].

$$A_{IP} = \frac{2\times(\sigma_{ys})_{45^o} - [(\sigma_{ys})_{0^o} + (\sigma_{ys})_{90^o}]}{2\times(\sigma_{ys})_{45^o}} \quad (2.4)$$

$$\delta = \frac{(P_{ct}.El)_{0^o} - (P_{ct}.El)_{90^o}}{(P_{ct}.El)_{0^o} + (P_{ct}.El)_{90^o}} \quad (2.5)$$

Where, $P_{ct}.El$ = % elongation.

2.5.2. Fatigue behaviour

Total strain amplitude ($\Delta\varepsilon_t/2$) controlled Low Cycle Fatigue (LCF) tests at room temperature were performed using Instron 8800 servo-electric test system, shown in Fig.2.4 (a)**.** LCF tests were conducted as per ASTM E606 standard in fully reversed (R= -1) condition using triangular waveform axial loading at constant strain rate ($\dot{\varepsilon}$), as given in Fig. 2.4(d). The LCF tests were performed at fixed strain amplitude (±0.5%) and strain rate (5×10^{-3} s^{-1}). Cylindrical LCF specimens with gauge diameter of 6 mm and 18 mm length and threaded ends of M12 x 1.75 mm (on either side), and radii of curvature of 24 mm were machined. Figs. 2.4(b and, c) show the dimensions of the cylindrical specimen and polished fatigue specimen used for the low cycle fatigue testing. The specimens were finished by fine machining and polishing to an average roughness of 0.5µm. Strain measurement was done using room temperature extensometer with gauge length of 12.5 mm and travel range of ±20%. The tests were conducted till failure of the specimen. For repeatability of fatigue results, two samples were tested at each condition. Fatigue fracture surfaces of the tested specimens were analysed using scanning electron microscope operating at 20kV.

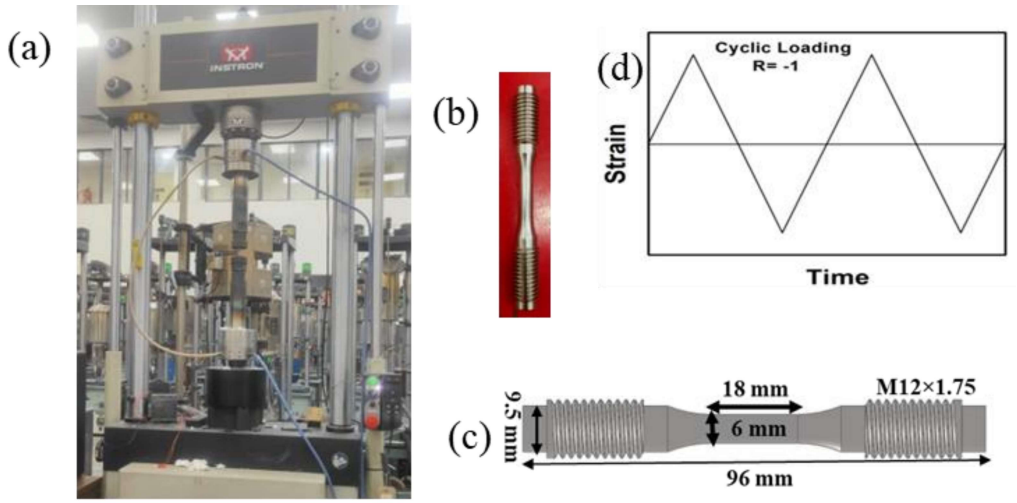

Fig. 2.4 (a) 100kN fatigue testing system (b) Polished fatigue sample (c) Geometry of fatigue sample (d) Triangular, fully reversed waveform for axial loading.

2.6. TRIBOLOGICAL BEHAVIOUR

2.6.1 Wear behaviour

At room temperature, the wear characteristics of AM and conventional maraging steel in as-built/as-received and heat-treated conditions were studied under sliding conditions. To conduct the wear test, a pin on disc (PoD) tribometer setup (Magnum) was utilised, as shown in Fig. 2.5 (a). The ASTM G99-17 standard was used to conduct wear tests at room temperature in 0^o, 45^o and 90^o oriented AM specimens and conventional maraging steel in their as-received and heat-treated conditions. Cylindrical samples of 30 mm length and 4 mm diameter were machined using wire-EDM, and are shown in Fig.2.5(b). 65 HRC EN31 steel was used for the counter disc. Samples were polished up to 2500 fine emery papers followed by cloth polishing. The average surface roughness of samples that were polished was found to be 160±10 nm. The counter disc and pin samples were cleaned with acetone before and after the test. The weight of the pin sample was determined using a METTLER TOLEDO balance with a least count of 0.1 mg. Tribology

tests were conducted for 16 minutes with applied loads of 20 N, 40 N, and 80 N, sliding distance of 480 m, sliding velocity of 0.5 m/sec, and worn track diameter of 40 mm. The weight loss was measured manually by comparing the weight before and after the test. The coefficient of friction was determined using data collecting software connected to the tribometer. The tribological statistics were expressed in terms of wear volume, wear coefficient and friction coefficient. Each test was performed three times for checking the reproducibility of the results. The wear volume is the volume loss of material per unit density, whereas the coefficient of friction is frictional force divided by normal force.

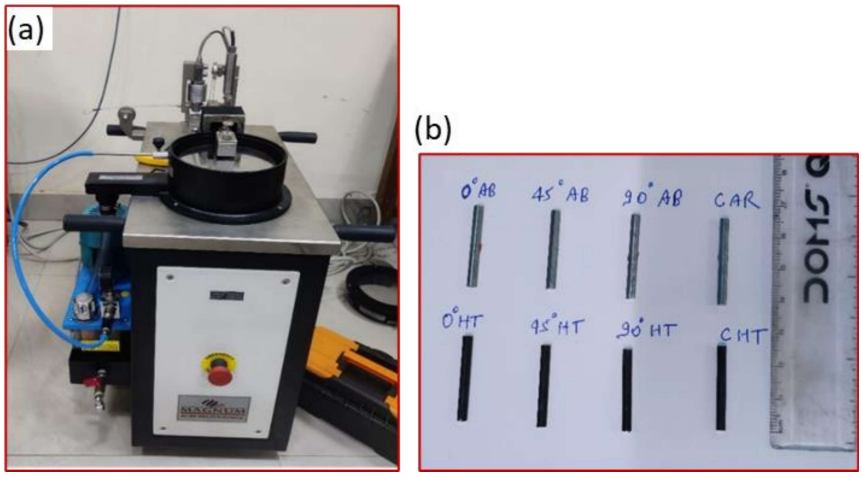

Fig. 2.5 (a) Pin on Disc (PoD) tribometer setup and (b) samples in different conditions.

The wear rate, Q (mm^3/m) was calculated using equation (2.6) [116].

$$Q=V/L \qquad (2.6)$$

where V is volume loss (in mm^3) and L is sliding distance (m) which was constant (480 m). As per Archard law, V is inversely proportional to hardness (H) as shown in equation (2.7).

$$V= kWL/H \qquad (2.7)$$

Where k is coefficient of wear and W is applied load.

In order to understand the wear mechanism, worn surface texture studies were carried out using FE-SEM (Nova Nano SEM 450) attached with EDS and Atomic force microscopy (AFM) using INTEGRA Prima microscopy.

2.6.2 Solid Particle Erosion behaviour

Air jet erosion tester (TR-471-800, DUCOM Bengaluru, India) was used to examine the solid particle erosion behaviour of AM and conventional maraging steel in as-received and heat-treated conditions. The machine is shown in Fig. 2.6(a). Wire-EDM was used to cut test samples of standard size ($25\times25\times5$ mm^3) from 0^o, 45^o, and 90^o oriented AB plates. Samples were paper and cloth polished using alumina suspension (R_a=0.2 μm) in accordance with the ASTM G-76-95 standard at room temperature, and tested sample shown in Fig. 2.6(b). In order to determine the erodent discharge rate, the mass of erodent discharged via nozzle for 10 minutes was collected. With the double-disc approach, the impact velocity of the erodent was calibrated. Process parameters of the erosion test are as follows, Erodent discharge rate: 4.5 g/min, Air pressure: 2.7 bar, Air and erodent discharge velocity: 100 m/sec, Impact angle: 90^o, Nozzle diameter: 3 mm. Fig. 2.6(c) shows that the erodent particles (Al_2O_3) are angular and uneven in shape, with sharp cutting edges. The average size of erodent particles was 45 μm. The surface of the material was impacted at 90^o by a sandblast-type erosion tester, capable of eroding material using compressed air stream and accelerated erodent. After 10 minutes, the weight loss was recorded, and after 40 minutes, the erosion rate ($g\ g^{-1}$) was determined using Equation 2.8, [117].

$$\text{Erosion Rate} = \frac{\text{Weight loss of target specimen}}{\text{Weight of erodent particle impinging on the target specimen}} \qquad (2.8)$$

In order to understand the erosion mechanism, eroded surface texture studies were carried out using FE-SEM (Nova Nano SEM 450) attached with EDS.

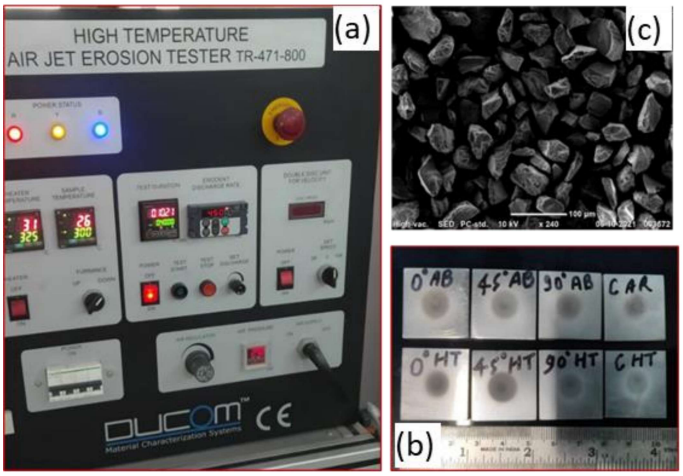

Fig. 2.6 (a) DUCOM air jet erosion system (b) Eroded samples in different conditions (c) Morphology of erodent particles.

2.7 CORROSION BEHAVIOUR

Using a three-electrode cell, electrochemical experiments were performed using a Potentiostat (CorrTest CS350) as shown in Fig. 2.7(a). The corrosion samples of dimensions 15×15×2 mm^3 were machined using wire-EDM from 0°, 45° and 90° oriented AM for corrosion testing. The samples were mirror polished, ultrasonically cleaned and air-dried as shown in Fig. 2.7(b).

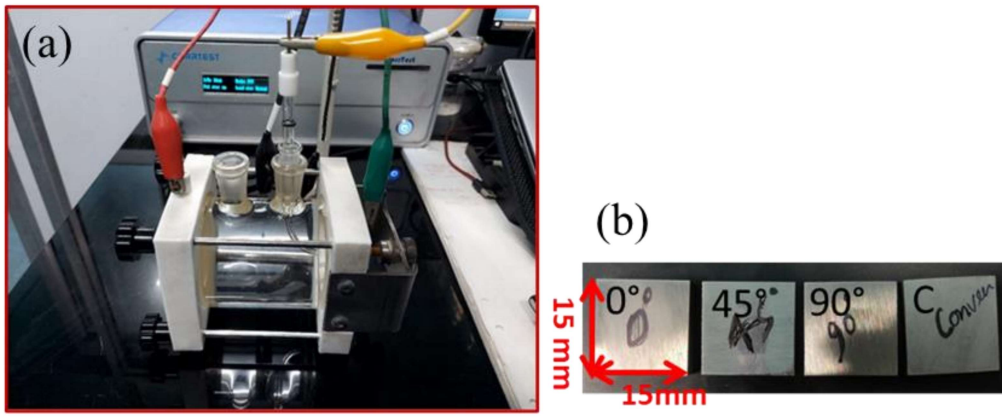

Fig. 2.7 (a) Electrochemical experimental setup (b) Polished AB samples in different orientations along with the conventional samples used for corrosion testing.

The working electrode was the test specimen, with an exposed area of 1 cm^2, counter and reference electrodes consisted of platinum wire mesh and saturated Ag/AgCl respectively. At a constant pH, electrochemical experiments were conducted at room temperature in a 3.5% NaCl solution. In order to obtain a constant open circuit potential (OCP), each sample was submerged in the NaCl solution for 3600 seconds. At a scan rate of 0.5 mV/s, potentio-dynamic polarization tests were performed, ranging from 1 V below OCP to +0.5 V above OCP. In order to assure reproducibility, experiments were conducted at least three times, under identical conditions, using fresh 3.5% NaCl electrolyte for each experiment. After stabilising the OCP, Electrochemical Impedance Spectroscopy (EIS) tests were performed on each sample. The signal's frequency spanned between 10 mHz and 100 kHz, and its amplitude was 10 mV relative to the OCP. The impedance results were expressed by Nyquist and Bode plots and analysed using the software CS studio 5 to find equivalent circuit, which characterizes the corroded layer formed on the samples. Every Nyquist plot consists of both inductive and capacitive loops. Typically, an electrical double layer is expressed as a capacitance component, but when the dispersion effect is taken into consideration, a constant phase angle element QPE_1, is substituted for the capacitance. The expression for the impedance of QPE is as per following Equation 2.9 [118].

$$Z = \frac{1}{\gamma(jw)^n} \qquad (2.9)$$

Where γ is a constant with unit $\Omega^{-1}.cm^{-2}$, exponent n is slope of bode plot whose values lie between 0 and 1, and *w* is the angular frequency. The value of n is 0, 1 and -1 represents a pure resister, pure capacitor and pure inductor respectively. The entire impendence of the model can be expressed as per following Equation 2.10.

$$Z = R1 + \frac{1}{\gamma(jw)^{n1} + \frac{1}{R2 + \frac{1}{1/jwL + \frac{1}{R3}}}} \qquad (2.10)$$

where R_1, R_2, and R_3 are the solution resistance, charge transfer resistance and intermediate polarization resistance respectively.

The corrosion products formed on the samples were characterised by X-ray photoelectron spectrometer (Thermo Fisher Scientific K-alpha system) using a monochromatic K_α source at 1400.0 eV, and the X-ray photoelectron spectra (XPS) data were collected. As a reference, the C_{1s} peak at 284.8 eV was used to correct the binding energy scale. Typically, a Gaussian component was utilised for curve fitting and the Shirley baseline method was used for the subtraction of background [119]. Further, using high-resolution scanning electron microscopy (FESEM, FEI QUANTUM 200 F) coupled with Energy Dispersive Spectroscopy (EDS), the surfaces of corrosion-tested samples were examined.

2.8 CHAPTER SUMMARY

The present chapter describes the materials of present investigation, processing methods, printing parameters, heat treatment, testing methods and characterization techniques used to study tensile, fatigue, tribological and corrosion behaviour of additive manufactured M300 steel in different orientations and the conventionally manufactured maraging steel.